

Absorption spectrum analysis based on singular value decomposition for photoisomerization and photodegradation in organic dyes

Yutaka Kawabe^{*a}, Toshio Yoshikawa^a, Toshifumi Chida^a, Kazuhiro Tada^a, Masuki Kawamoto^b, Takashi Fujihara^b, Takafumi Sassa^b, Naoto Tsutsumi^c

^aChitose Institute of Science and Technology, 758-65 Bibi, Chitose, Hokkaido, 066-8655 Japan

^bRIKEN, 2-1 Hirosawa, Wako, Saitama 351-0198, Japan

^cFaculty of Materials Science and Engineering, Kyoto Institute of Technology, Matsugasaki, Sakyo, Kyoto 606-8585, Japan

ABSTRACT

In order to analyze the spectra of inseparable chemical mixtures, many mathematical methods have been developed to decompose them into the components relevant to species from series of spectral data obtained under different conditions. We formulated a method based on singular value decomposition (SVD) of linear algebra, and applied it to two example systems of organic dyes, being successful in reproducing absorption spectra assignable to *cis/trans* azocarbazole dyes from the spectral data after photoisomerization and to monomer/dimer of cyanine dyes from those during photodegradation process. For the example of photoisomerization, polymer films containing the azocarbazole dyes were prepared, which have showed updatable holographic stereogram for real images with high performance. We made continuous monitoring of absorption spectrum after optical excitation and found that their spectral shapes varied slightly after the excitation and during recovery process, of which fact suggested the contribution from a generated photoisomer. Application of the method was successful to identify two spectral components due to *trans* and *cis* forms of azocarbazoles. Temporal evolution of their weight factors suggested important roles of long lifetimed *cis* states in azocarbazole derivatives. We also applied the method to the photodegradation of cyanine dyes doped in DNA-lipid complexes which have shown efficient and durable optical amplification and/or lasing under optical pumping. The same SVD method was successful in the extraction of two spectral components presumably due to monomer and H-type dimer. During the photodegradation process, absorption magnitude gradually decreased due to decomposition of molecules and their decaying rates strongly depended on the spectral components, suggesting that the long persistency of the dyes in DNA-complex related to weak tendency of aggregate formation.

Keywords: DNA complex, cyanine, azo, dye laser, photoisomerization, photodegradation, singular value decomposition, chemometrics

1. INTRODUCTION

Needless to say, optical spectroscopy is one of the most powerful tools for nondestructive probing of materials during temporal evolution under chemical reactions or dynamical physical processes. When multiple species of materials coexist in the system, optical absorption spectrum would be a linear combination of the spectra of constituting elements unless strong mutual interaction disturbs their additivity. If considering system is under temporal evolution and/or spatial inhomogeneity, it would be possible to gather huge number of spectral data made up by involving elements with wide variety of ratio. Once we can decompose the mixed spectra properly into those ascribed to species, the data would give rich information about the evolving process. It is possible to find out the number of incorporating materials in a system with a method based on linear algebra, which had been developed by researchers of analytical chemistry. And wide varieties of computational methods, collectively called as 'chemometrics', are now being strong tools for many types of chemical analyses involving spectral measurements.¹⁻³

* y-kawabe@photon.chitose.ac.jp; phone +81 123 27 6067; fax +81 123 27 6067

In this study, we applied the method of singular value decomposition (SVD) and supplemental calculation in order to find the spectra for involving species during photoisomerization process in azocarbazole dyes and photodegradation process in cyanine dyes embedded in DNA complex matrix.⁴ In the next section, theoretical framework will be given, in which are described a technique to construct physically realistic spectra from mathematically derived original decomposition as well as a brief description of SVD method, followed by its application to two examples. Short remarks about its possibility and limit will be given finally.

2. THEORETICAL

One spectral chart can be considered as a set of numerical values obtained at N wavelength points, the number of which will be determined by the resolution of detection devices or other technical conditions. In the context of linear algebra, the data set can be recognized as a point in N -dimensional (Euclidean) space. When M spectral data are obtained, the data set are considered as M points in N -dimensional space. If all spectra have the same shape, all points should lie along or scatter around a one-dimensional subspace, a line, defined in the whole space. It might be easy to determine the line by minimizing the summation over squared distance between the line and scattered data points. If spectra are composed of two elements, data would be located close to a plane spanned by two 'lines' and the determination of the plane can be achieved by some computational procedure of which detail was already described in our preceding work.⁴

Although the plane (or superplane with higher dimension) can be derived mathematically or automatically, there is no absolute way to determine molecular spectra in the plane without arbitrariness. In order to explain the concept, a schematic diagram is depicted in Fig. 1. Here, we assume that the spectra are composed of two components, for simplicity and also because the situation corresponds to our study. Spectral data for a binary composite will scatter in some region of N -dimensional superspace and nearly compose a two-dimensional subspace as shown with a gray plane in the figure which can be determined by purely mathematical procedure.^{4,5} Because the data points located close to the plane, their projection on to the plane reflects almost all original information except some contribution from noise.

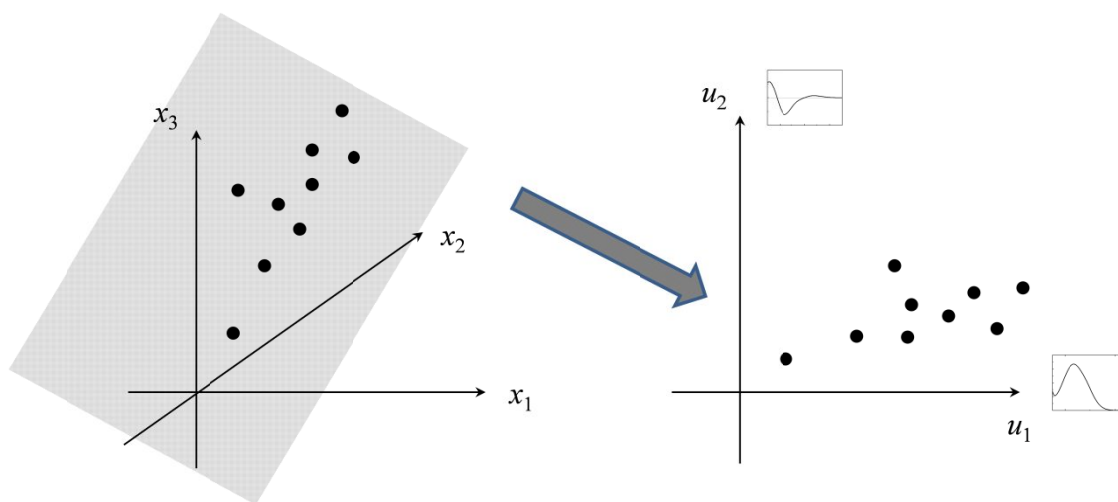


Figure 1. Spectral data would scatter in N -dimensional superspace, although only 3 axes can be indicated in the left figure. The optimized plane (assumed to be 2-dim. for binary mixture) indicated by a gray hatch can be determined mathematically. When the data points are projected on the plane, the spectral data can be expressed as points in a 2-dimensional plane composed of two axes (two spectra) as depicted in the right half.

From the SVD procedure over M data points, M singular values accompanied by a corresponding eigen vector (spectrum) can be obtained. Because singular values indicate the weight factor of the corresponding spectrum, the spectra with relatively large singular values should be selected as spectral components. Selected eigen spectra form an orthonormal basis of the plane, but the spectral set obtained in this way cannot give the spectra of incorporating molecules, because these eigen spectra are always be orthogonal to each other, thus inevitably include negative values which should be avoided for absorbance data. As shown on the axis u_1 in Fig. 1, the spectrum corresponding to the

maximum singular value would be all positive because all the original absorbance data are made up from positive values, but the second spectrum u_2 must have negative values in order to be orthogonal to u_1 .

Mathematically, all combinations of two vectors in the 2-dimensional plane can be a basis set as long as these are linearly independent. Some physically consistent guideline must be required to find out new axes (basis set). One necessary condition is that all components of axes have non-negative values, because they express absorption spectra for chemical components. We adopted a very simple algorithm to determine directions of axes where all N components are non-negative.

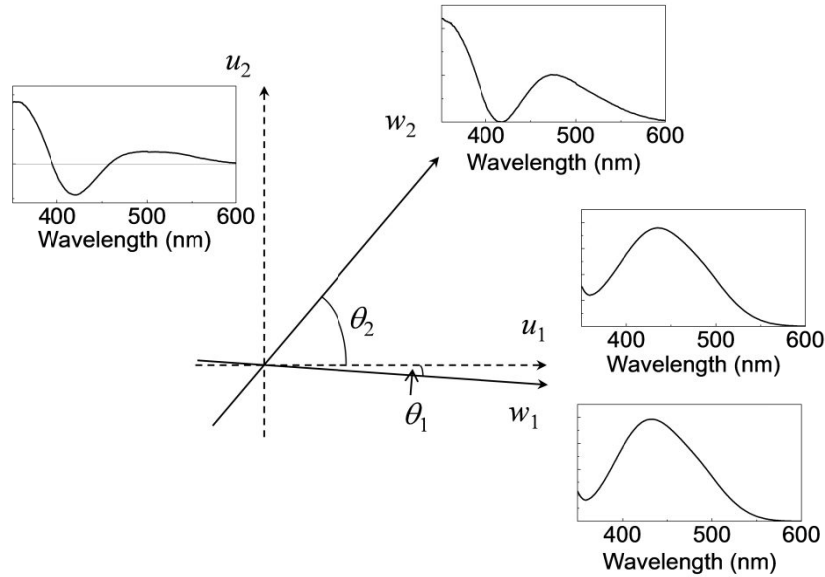


Figure 2. Example of analysis: Two orthogonal vectors u_1 and u_2 determined by SVD procedure define a plane. With the transformation led by eqs. (3a) and (3b), two axes w_1 and w_2 can be obtained. Actually, any combinations of two vectors lying between w_1 and w_2 can reproduce experimental data, being possible to be molecular spectra, but there is no rigorous way to determine 'real' molecular spectrum. The shapes of u_1 and w_1 are very similar because of their close directions.

In the following, we will find the region where the non-negative condition is satisfied. All vectors in the plane can be expressed as one parameter t , when neglecting the difference in norm because the length of the vector does not matter the sign of components. When u_1 , and u_2 are mathematically determined bases, their linear combination can be given as the following expression.

$$v = u_1 - t u_2 \quad (1)$$

In order for all v components to be positive, $u_{1,k} - t u_{2,k} > 0$ must be satisfied for all k (index for wavelength). Because $u_{1,k}$ is usually positive, the condition $t r_k < 1$ (where $r_k = u_{2,k}/u_{1,k}$) leads to the followings.

$$t < r_k^{-1} \quad \text{for } r_k > 0, \text{ and } t > r_k^{-1} \quad \text{for } r_k < 0 \quad (2)$$

Therefore, the parameter t must be in between two values r_1^{-1} and r_2^{-1} , where $r_1 = \max(r_k)$, and $r_2 = \min(r_k)$. By choosing these two boundary values of t for the determination of the axes, these normalized forms given as follows can be molecular spectra constituting mixture.

$$w_1 = \frac{r_1}{\sqrt{1+r_1^2}} u_1 - \frac{1}{\sqrt{1+r_1^2}} u_2 \quad (3a)$$

$$w_2 = -\frac{r_2}{\sqrt{1+r_2^2}}u_1 + \frac{1}{\sqrt{1+r_2^2}}u_2 \quad (3b)$$

The angle of w_1 and w_2 from axis u_1 can be obtained from the following expressions.

$$\sin \theta_1 = -\frac{1}{\sqrt{1+r_1^2}} \quad (4a)$$

$$\sin \theta_2 = \frac{1}{\sqrt{1+r_2^2}} \quad (4b)$$

An example obtained from the data in the next section is drawn schematically in Fig. 2. The results seem to reproduce the molecular spectra. As known from the algorithm, any vectors lying between w_1 and w_2 may be a molecular spectrum and no rigorous way to determine the ‘real’ spectra. The obtained spectrum would be one of the most probable candidates waiting for confirmation with another experimental or theoretical technique.

It is also important and interesting to extend the method to ternary, quaternary and more complex composites. However, it is not easy to find three axes most optimized in three-dimensional space with the same non-zero constraint.

3. TRANS-CIS PHOTOISOMERIZATION IN AZOCARBAZOLES

Azo-carbazole materials were considered to be promising for photorefractive and also for photochromic applications, being employed for the study of real time holography.^{6,7} Demonstration of updatable image storage promoted the development of real-time three-dimensional display, and it was partially achieved in a laboratory. In spite of their high performance, mechanism of optical constant modulation has not been clarified very well, although photoisomerization and following reorientation might play essential roles. In our development, azo-carbazole dyes named NACzEtOH (NACzE) and CACzEtOH (CACzE) have been used as chromophores doped in an inert polymer PMMA, because of their high performance and superior stability and easiness for thick film fabrications.^{8,9} Recently, we identified the long-lived *cis* state of NACzEtOH from the temporal evolution of absorption spectrum after the illumination with blue light and an analysis based on SVD described above.⁴

In this proceeding, we describe the details of the results for NACzEtOH and also for CACzEtOH for comparison. Thin film samples are formed by a spin coating from thin dimethylformamide solutions including both PMMA and the dye with the weight ratio of 7:3. After illumination with a randomly polarized light of absorption peak wavelength, absorption spectrum was monitored during half an hour giving a number of spectral charts for analysis. Fig. 3 displays the two components extracted from 33 frames obtained before and after the blue light illumination for NACzEtOH. The principal component (component 1) had a peak at 434 nm and the next component had at 473 nm.

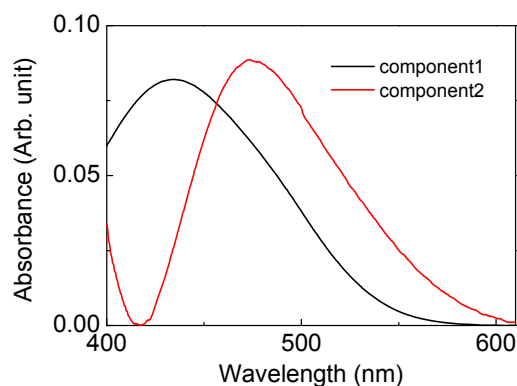


Figure 3. Spectra of two components obtained from series of absorption spectra of NACzEtOH obtained before and after light illumination.

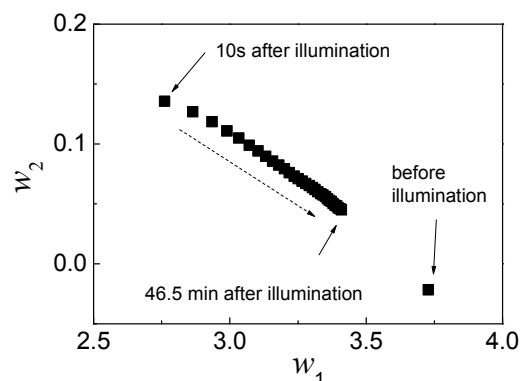


Figure 4. Plot of spectral components w_1 and w_2 obtained from SVD analysis for NACzEtOH.

Because all spectra were approximated by the linear combination of two components, each data point can be plotted in two-dimensional plane defined by spectra w_1 and w_2 , as depicted in Fig. 4. The initial point locates close to the abscissa, meaning that the spectrum was mainly made up with w_1 component. Light illumination induced a jump to the leftmost point followed by gradual recovery to the initial point. Complete recovery was not achieved, because experiment was terminated after 45 minutes. The fact that all points lie on a straight line means that recovery of w_1 component and reduction of w_2 component behaved with the same manner. Their temporal decay was shown in Fig. 5, showing non-exponential but temporally evolved with the similar way. Indeed, the ratio of two components was between 6.6 and 7.1 along the process. If the system can be described by two states as *trans* and *cis*, the ratio would be a constant. In this case, these two states were dominant absolutely, and slight discrepancy may indicate little contribution from the third state as *trans* molecules with axis perpendicular to the sample plane as we suggested in our former study.

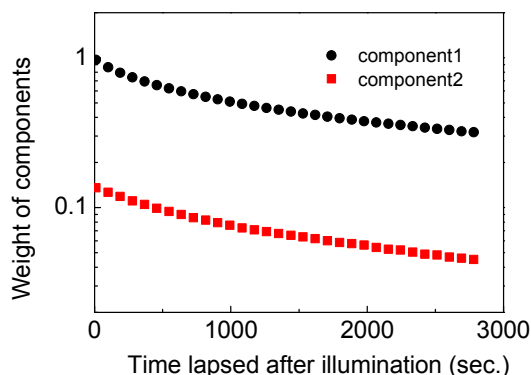


Figure 5. Temporal evolution of two components (w_1 and w_2) in NACzEtOH spectra.

The same analysis was applied to CACzEtOH of which data was composed six spectra obtained in the similar procedure. The crude data showing strong reduction due to excitation and gradual recovery in time (given in the left panel of Fig. 6) was processed to give two components shown in the right panel of Fig. 6. Peak wavelengths of these components located at 419 nm and 467 nm, which were slightly shorter than those for NACzEtOH, reflecting the blue shift of the peak in experimental data due to weakness of the acceptor. Although only six spectra were involved in the calculation, quality of the decomposition did not get worse.

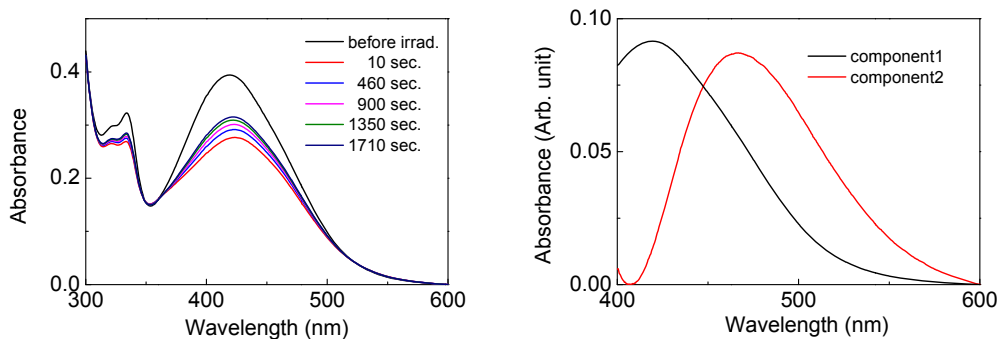


Figure 6. (left) Absorption spectra of CACzEtOH doped film observed before and after light illumination, and (right) two components obtained from the spectra with SVD analysis.

Weight factor for the experimental data is plotted in Fig. 7, where we employed original coordinate determined by orthogonal basis spectrum set u_1 and u_2 . The point corresponding to the spectrum before illumination locates distantly from others. Blue light illumination moved it to left lower position followed by gradual returning to the initial place while the experiment was terminated on midway, and the behavior was consistent with the evolution depicted in Fig. 6 (left).

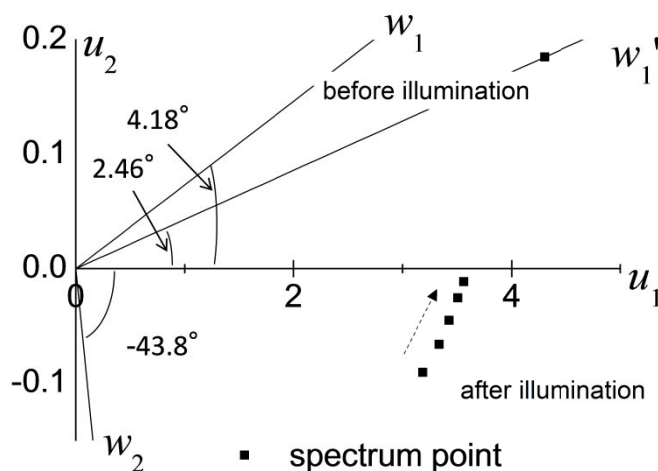


Figure 7. Plot of spectral components for CACzEtOH depicted in u_1 - u_2 plane as well as axes obtained from the transformation to w_1 - w_2 basis.

In Fig. 7, the new axes determined with the procedure given in section 2 were drawn on u_1 - u_2 plane. The w_1 axis corresponding to the spectrum of principle component directs about 4 degree from u_1 axis. The spectrum before illumination slightly deviates from w_1 , leading to two possible interpretations. If w_1 and w_2 exactly reflect the spectra of molecules, the sample before illumination must have included two components, that is, *trans* and *cis*. If one can believe that only the *trans* molecules contributes to the initial spectrum, one axis w_1' must be defined from the initial point as given in Fig. 7. Because there was no remarkable difference between the spectral shapes of w_1 and w_1' , it was difficult to find out more adequate conjecture only from the data. Here, we assumed that spectra could be decomposed into w_1' and w_2 , and time dependence of the weight factors are plotted in Fig. 8 which showed the similar decay and recovery profiles for both components suggesting that no intermediate states like perpendicularly oriented *trans* molecules exist. Comparison to NACzEtOH indicates that much slower evolution was observed in CACzEtOH which showed longer lifetime of *cis* state due to weakness of acceptor effects.

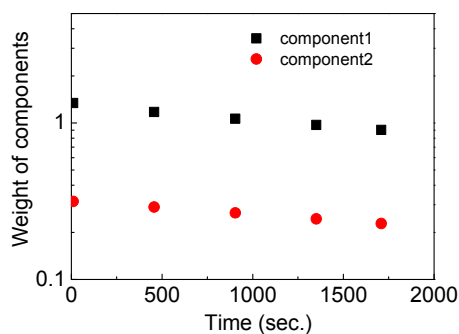


Figure 8. Temporal evolution of two components (w_1 and w_2) in CACzEtOH spectra

We need to remark arbitrariness associated to the selection of spectral region. Honestly speaking, results depend somewhat on how data are treated. Most important factors are spectral range and zero position. In our analysis, 400 – 610 and 400 – 600 nm were selected for NACzEtOH and CACzEtOH, respectively. The peak positions did not depend so strong with the ranges. These ranges were selected in order to utilize the broadest range as long as the effect from the matrix could be avoided. The range as well as zero base line affects the structure of the space spanned by u_1 and u_2 and also axis directions determined by w_1 and w_2 . Sometimes consideration based on physics should be applied for modification as shown in Fig. 7, because mathematical scheme does not automatically choose physically justified solutions. In spite of some arbitrariness, the fact that obtained spectra and decay plots did not strongly depend on the choice of data made this method promising for the spectroscopic studies on organic functional materials.

4. DEGRADATION OF CYANINE DYES DOPED IN DNA COMPLEX

Combination of DNA-surfactant complex and organic dye induces interesting optical features useful for electronic and/or photonic devices via exotic interaction among the constituents. In particular, enhancement of fluorescence yield encourages the application of the materials to tunable lasers or organic light emitting diodes.¹⁰⁻¹² We have doped several types of cyanine dyes into DNA complex, demonstrating light amplification and laser action under optical pumping.¹³⁻¹⁷ Our preceding studies showed that durability of the lasing dyes was apparently extended due to DNA-complex matrix compared to those doped in conventional polymers.^{14,16,17} Efficient laser performance, superior durability and compatibility to wide range of fabrication methods indicate that the materials would be promising for thin film tunable laser devices.^{15,17-20} Interaction of dye and DNA are considered to play an important role for high durability and good performance, since the specific DNA structure could protect the dyes from moist environments. Indeed, our recently developed devices showed a long durability up to 1 hour under relatively strong optical pumping.²¹ Therefore, it is important to study their interaction configurations and degradation mechanism for further improvement and development of micro-sized tunable thin-film lasers. In this section, we describe the investigation of the degradation of several cyanine (or carbocyanine) dyes doped in DNA-surfactant complex used in our preceding studies on optical amplification and lasing.¹⁷ Dye degradation process was probed as variation of absorption spectral shape induced by optical excitation. Results from the SVD analysis are given, determining composing spectral elements.

Molecular structures for the compounds used in this study are shown in Fig. 9. The dye molecules has been known as cyanine or DiQC₂(1) if $n = 1$ and carbocyanine or DiQC₂(3) if $n = 3$, and has been used for staining DNA for biological researches and also their nonlinear optical activities has attracted attention.^{22,23} The dye has absorption peak at about 530 nm for DiQC₂(1) and 610 nm for DiQC₂(3) due to long polymethine chain between two aromatic rings. As a surfactant composing the complex we employed cetyltrimethylammonium (CTMA), the most popular material for DNA based functional devices.^{10,11} Synthesis method for the complex and the technique for film formation have been described in our preceding works.^{13,17} In this study, several samples were fabricated with the concentration of the dyes adjusted to be 1/20 molar ratio when one base pair and two surfactant molecules are counted as a unit. The value means 1.9 wt% for DiQC₂(1) and 2.0 wt% for DiQC₂(3). Thickness of the films were evaluated to be 4 ~ 5 μm with a surface profiler.

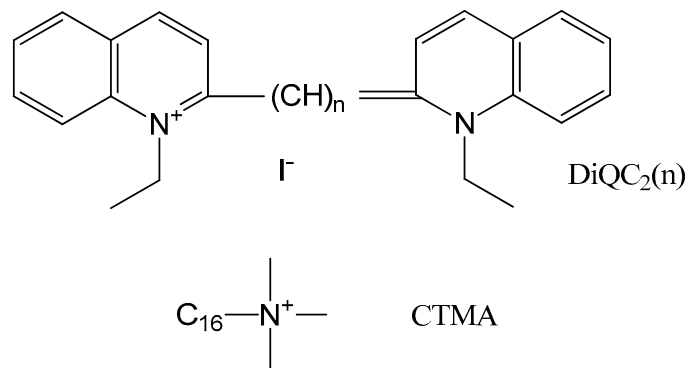


Figure 9. Molecular structure of DiQC₂(1) cyanine and DiQC₂(3) carbocyanine iodide dyes and CTMA used for experiments.

Degradation was caused by continuous irradiation with a pulsed laser light from a frequency-doubled Q-switched Nd:YAG laser operating at 10 Hz. For the measurements of absorption spectra of the degraded films, a commercial UV/Vis absorption spectrometer was used. Measurements were made after every half minute irradiation during which the fluence was 12 mJ/cm² per pulse. Energy density injected during each cycle was 3.6 J/cm² and the total fluence during 10 min. irradiation was 72 J/cm². The same experiment was made also for the sample composed of the dyes and inert polymer polymethylmethacrylate (PMMA) for comparison.

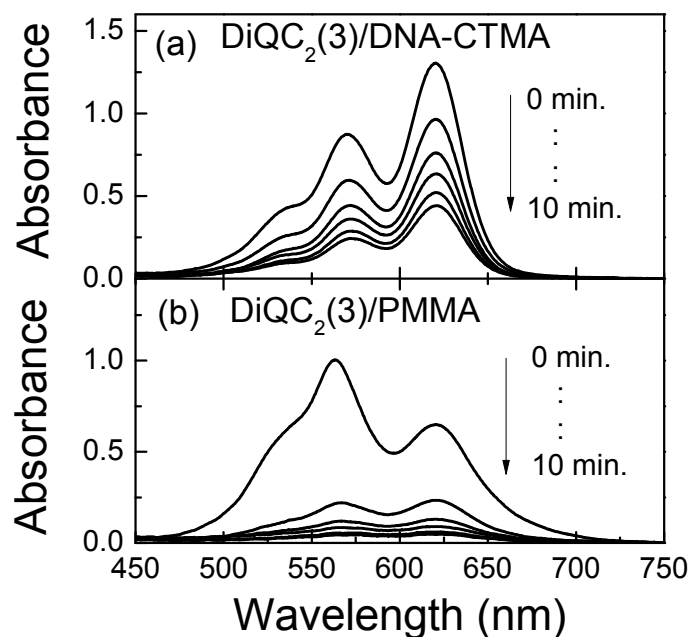


Figure 10. Evolution of spectral shape under optical pumping for DiQC₂(3) embedded in (a) DNA-CTMA and (b) PMMA. Six among twenty-one spectra are selected to give concise views.

Evolution of spectra obtained for the DiQC₂(3) was given in Fig. 10 for DNA-CTMA and PMMA matrices. As known from the figures, initial shape of the spectrum was different from each other. For the case of DNA-CTMA matrix, the curve gives a typical spectral feature of cyanine dyes composed of principal peak accompanied by several vibronic bands, while high energy peak was enhanced when embedded in PMMA. During the degradation process, change of spectral shape was less significant for the case of DNA complex, but it was quite remarkable for the PMMA sample. After 10 minute irradiation, however, both spectral shapes became similar. From the result, we can provide a simple phenomenological model for the degradation process in the matrices. The change of the spectral shape for the PMMA

sample can be attributed to the contribution from multiple components with different degradation rates. For the case of DNA complex, the shape was more static because there was one dominant component. In order to find these components, the same SVD procedure was applied.

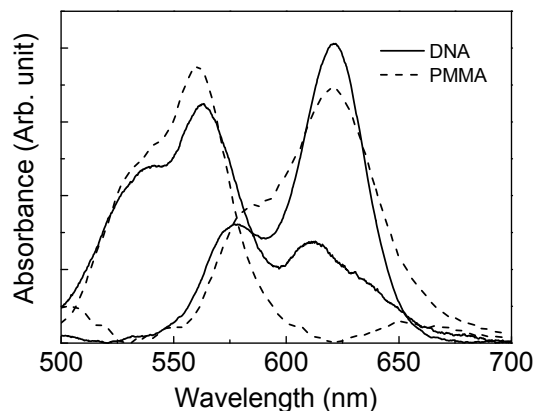


Figure 11. Extracted spectra for $\text{DiQC}_2(3)$ in DNA complex (solid curves) and in PMMA (dashed curves).

With the method, we have decomposed the spectra into two components shown in Fig. 11 where the magnitude of each spectrum was normalized. For both cases, similar decomposition was achieved giving peaks around 620 nm and 560 nm. The curve for DNA complex with shorter wavelength main peak has a secondary one at 610 nm. Although this kind of secondary peak can be eliminated by adjusting the spectral range and base line, we left it as obtained because it was difficult to ensure the validity of such modification from the principle of physics.

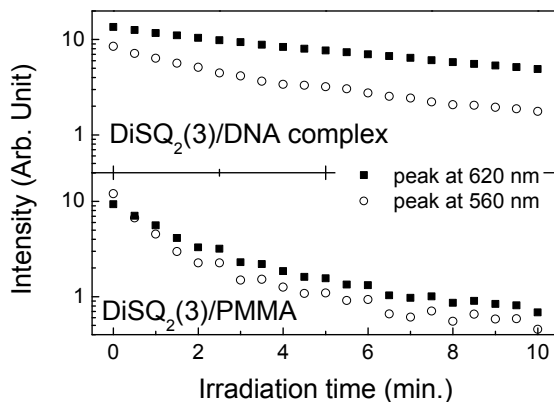


Figure 12. Temporal evolution of the magnitudes of the spectral components given in Fig. 4 for $\text{DiSQ}_2(3)$ in DNA-CTMA and in PMMA.

The evolutions of two components during degradation are shown in Fig. 12. For the case of DNA complex, contribution from the main peak (620 nm) was always greater and its durability was superior. On the other hand, both components degraded faster in PMMA matrix than in DNA complex, but still long durability for the peak at 620 nm was observed. In other words, component having a shorter wavelength peak showed quicker decay for the both cases. We also made the same analysis for the case of $\text{DiQC}_2(1)$. It was impossible, however, to separate the spectra, because there was less remarkable change of the spectral shape during irradiation.

From the results, the absorption spectra of $\text{DiQC}_2(3)$ were found to consist of at least two components. One locating in the longer wavelength side had typical spectral shape of the absorption always observed for cyanine dyes accompanying vibronic sub-bands. The other one situating in high energy side also gave similar structure. Decaying rate under optical pumping was faster for the latter one for both cases. Assuming that the purity of the dopant did not depend on matrix,

two spectral components should reflect the structural or electronic-state changes of the dopant through intermolecular interactions. Most probable reason is the formation of dimer which shifts the absorption band higher or lower energy sides depending on the relative position of two identical molecules. As known from the theory of molecular exciton, each molecular electronic level splits into two states in dimer due to intermolecular interaction.²⁴⁻²⁶ When two linearly conjugated molecules like cyanines align vertically (making head-to-tail coupling), the lower state is electric-dipole allowed and the other forbidden, giving strong absorption in red side showing a state called 'J' of dimer. On the contrary, 'H' type dimer band will appear in high energy side if molecules align side by side.

It has been well known that cyanine and other organic dyes form dimer and other complicated aggregates when these are dissolved in some solvents with high concentration.²⁷⁻²⁹ Usually the determination of H-type dimer spectrum was not so easy because the vibronic bands of monomer always overlapped to the dimer states. In this study, we succeeded to separate two components with the mathematical procedure, making it possible to define the shape of dimer spectrum and to evaluate the intermolecular interaction energy determining the splitting of the lowest excited state. For DiQC₂(3) in PMMA and DNA complex, it was evaluated to be 1,500 cm⁻¹, the value was consistent to those predicted from preceding theoretical and experimental studies.³⁰

It is possible to get insight into the role of DNA complex for durability of carbocyanine dyes. In the spectrum for the PMMA matrix, the dimer was found to be more significant in population than the case of DNA complex, and the dimer had low resistance to light irradiation. Therefore, one important role of DNA was to prevent the formation of dimer or other aggregates which showed up in PMMA matrix. Our former study revealed that small amounts of DNA stimulate dye aggregation, but excess amounts enhance the DNA-dye interaction reducing the dye aggregation, and such behavior was attributed to ionic interaction among constituents.²⁸ From this study, it is suggested that ionic character of DNA-CTMA would suppress the formation of dimer, leading to relatively long lifetime of the dye because dimer was more easily degraded by the optical pumping. Of course, the details of how DNA, surfactant and cationic dye interact were not well known. Our results indicate that controlling of intermolecular interaction can help us to manufacture more practical optical devices such as compact dye lasers based on DNA complex.

5. CONCLUSION

In order to analyze the absorption spectrum of organic mixtures, a mathematical procedure based on singular value decomposition was formulated and applied to two systems. From multiple spectra of polymer films highly doped with azo-carbazoles obtained before and after light illumination, two components assignable to *trans* and *cis* states were identified. Long lifetime of the *cis* states of the dyes found from the analysis is considered to be one reason for high holographic performance of the dyes. From the photodegradation processes in a carbocyanine dye embedded in DNA complex, two species assignable to monomer and dimer states were spectrally decomposed. Obtained profiles of temporal decay suggested that high durability of the dye in the complex could be due the prevention of dimerization. These two examples gave evidence of the availability of the method, although the mathematical process does not assure the rightfulness based on physical and/or chemical principles. The method would be a strong tool for spectroscopic studies if applied adequately.

ACKNOWLEDGEMENT

This work was partially supported by the program for Strategic Promotion of Innovative Research and Development (SPIRE), Japan Science and Technology Agency (JST).

REFERENCES

- [1] Cuesta Sánchez, F., van den Bogaert, B., Rutan, S. C. and Massart, D. L., "Multivariate peak purity approaches," *Chemometrics Intell. Lab. Syst.* **34**, 139-171 (1996).
- [2] de Juan, A. and Tauler, R., "Chemometrics applied to unravel multicomponent processes and mixture. Revisiting latest trends in multivariate resolution," *Anal. Chim. Acta* **500**, 195-210 (2003).
- [3] Garrido, M., Ruis, F. X. and Larrechi, M. S., "Multivariate curve resolution-alternating least squares (MCR-ALS) applied to spectroscopic data from monitoring chemical reaction processes," *Anal. Bioanal. Chem.*, **390**, 2059-2066 (2008).

- [4] Yoshikawa, T., Kawamoto, M., Fujihara, T., Tada, K., Sassa T. and Kawabe, Y., "Long-lived cis state of azocarbazole dye with strong acceptor highly doped in a polymer matrix," *J. Opt. Soc. Am. B* **23**, 622-627 (2015).
- [5] Strang, G., [Linear Algebra and Its Applications], Academic Press, (1976).
- [6] Tsutsumi, N., Kinashi, K., Sakai, W., Nishide, J., Kawabe, Y. and Sasabe, H., "Real-time three-dimensional holographic display using a monolithic organic compound dispersed film," *Opt. Mater. Express* **2**, 1003–1010 (2012).
- [7] Tsutsumi, N., Kinashi, K., Tada, K., Fukuzawa, K. and Kawabe, Y., "Fully updatable three-dimensional holographic stereogram display device based on organic monolithic compound," *Opt. Express* **21**, 19880–19884 (2013).
- [8] Nishide, J., Tanaka, A., Hirama, Y. and Sasabe, H., "Non-electric field photorefractive effect using polymer composites," *Mol. Cryst. Liq. Cryst.* **491**, 217–222 (2008).
- [9] Kawabe, Y., Fukuzawa, K., Uemura, T., Matsuura, K., Yoshikawa, T., Nishide, J. and Sasabe, H., "Photoinduced grating formation in a polymer containing azo-carbazole dyes," *Appl. Opt.* **51**, 6653–6660 (2012).
- [10] Jin, J.-I. and Grote, J., eds., [Materials Science of DNA] CRC Press, Boca Raton (2012).
- [11] Kwon, Y.-W., Lee, C. H., Choi, D.-H. and Jin, J.-I., "Materials Science of DNA," *J. Mater. Chem.* **19**, 1353-1380 (2009).
- [12] Kobayashi, N., Ouchen, F. and Rau, I., eds., [Nanobiosystems: Processing, Characterization, and Applications VI], *Proc. SPIE* 8817 (2013).
- [13] Kawabe, Y., Wang, L., Nakamura, T. and Ogata, N., "Thin-film lasers based on dye-deoxyribonucleic acid-lipid complexes," *Appl. Phys. Lett.* **81**, 1372-1374 (2002).
- [14] Chida, T. and Kawabe, Y., "Hemicyanine-DNA-complex: application to solid-state dye lasers," *Nonlin. Opt. Quant. Opt.* **45**, 85-91 (2012).
- [15] Chida, T. and Kawabe, Y., "Transient grating formation in azo-doped polymer and its application to DNA-based tunable dye laser," *Opt. Mater.* **36**, 778-781 (2014).
- [16] Honda, M., Nakai, N., Fukuda, M. and Kawabe, Y., "Optical amplification and laser action in cyanine dyes doped in DNA complex," *Proc. SPIE*, **6646**, 664609 (2007).
- [17] Chida, T. and Kawabe, Y., "Tunable DFB dye lasers based on DNA-surfactant complexes," *Proc. SPIE*, **8464**, 84640E (2012).
- [18] Sznitko, L., Mysliwicz, J., Karpinski, P., Palewska, K., Parafiniuk, K., Bartkiewicz, S., Rau, I., Kajzar F. and Miniewicz, A., "Biopolymer based system doped with nonlinear optical dye as a medium for amplified spontaneous emission and lasing," *Appl. Phys. Lett.* **99**, 031107 (2011).
- [19] Mysliwicz, J., Sznitko, L., Sobolewska, A., Bartkiewicz S. and Miniewicz, A., "Lasing effect in a hybrid dye-doped biopolymer and photochromic polymer system," *Appl. Phys. Lett.* **96**, 141106 (2011).
- [20] Yu, Z., Li, W., Hagan, J. A., Zhou, Y., Klotzkin, D., Grote J. G. and Steckl, A. J., "Photoluminescence and lasing from deoxyribonucleic acid (DNA) thin films doped with sulforhodamine," *Appl. Opt.* **46**, 1507-1513 (2007).
- [21] Suzuki, T. and Kawabe, Y., "Light amplification in DNA-surfactant complex films stained by hemicyanine dye with immersion method," *Opt. Mater. Express* **4**, 1411–1419 (2014).
- [22] Waring, M. J. and Chaires, J. B., eds., [DNA binders and related subjects], Springer, Berlin (2005).
- [23] Kobayashi, T., ed., [J-aggregates vol. 2], World Scientific, Singapore (2012).
- [24] Davydov, A. S., [Theory of Molecular Excitons], Plenum, New York (1971).
- [25] Agranovich, V. M., [Excitations in Organic Solids], Oxford Univ. Press, Oxford (2009).
- [26] Pope, M. and Swenberg, C. E., [Electronic Processes in Organic Crystals and Polymers, 2nd ed.], Oxford Univ. Press, Oxford (1999).
- [27] Seifert, J. L., Connor, R. E., Kushon, S. A., Wang, M. and Armitage, B. A., "Spontaneous assembly of helical cyanine dye aggregates on DNA nanotemplates," *J. Am. Chem. Soc.* **121**, 2987-2995 (1999).
- [28] Kawabe, Y. and Kato, S., "Spectroscopic study of cyanine dyes interacting with the biopolymer, DNA," *Dyes and Pigments*, **95** 614-618 (2012).
- [29] Daltrozzo, E., Scheibe, G., Gschwind, K. and Haimerl F., "On the structure of the J-aggregates of pseudoisocyanine," *Photogr. Sci. Eng.* **18**, 441-450 (1974).
- [30] Kasha, M., Rawls, H. R. and Asharf El-Bayoumi, M., "The exciton model in molecular spectroscopy," *Pure Appl. Chem.* **11**, 371-392 (1965).